

HYDRATION OF THE MARTIAN SURFACE: WHAT WE CAN LEARN FROM ORBIT. J. Audouard^{1,2}, F. Poulet², M. Vincendon², R. E. Milliken³, J.-P. Bibring² and A. D. Rogers¹, ¹Stony Brook University, NY, USA, ²Institut d'Astrophysique Spatiale (UPSUS/CNRS) Orsay, France; ³Dept. Geological Sciences, Bown University, Providence, RI, USA. Contact: joachim.audouard@stonybrook.edu

Introduction: Several reservoirs of water have been identified on Mars. We investigate one of them, the hydration of the Martian regolith and rocks, probed by a broad spectroscopic absorption near $\sim 3 \mu\text{m}$ caused by H_2O molecules and $-\text{OH}$ terminal groups bound at various energy to solid substrates in the first few μm of the regolith materials. This “ $3 \mu\text{m}$ absorption” was early remarked in spectroscopic infrared (IR) remote-sensing observations of the Martian surface [1, 2, 3] and is seen in every ice-free spectra of modern IR orbital datasets such as OMEGA/MEx and CRISM/MRO [4, 5].

Usually, the hydration of the regolith materials is seen as either “structural”, if H_2O and $-\text{OH}$ are part of the minerals structure (e.g. in hydrous minerals such as phyllosilicates and sulfates), or “adsorbed”, if the water molecules are available for exchanges with the atmosphere (given the atmospheric variations of relative humidity and water vapour). Adsorbed water can be bound at variable energy to the substrate, depending on the composition (and defects) and given the relative humidity and water vapour content above the surface. In the case of Mars, the implication of the surface hydration in the global water cycle is still in debate. The seasonal and diurnal variations of water vapour in the atmosphere [6, 7, 8] and water cycle simulations [9, 10] have either hint towards or excluded an important role of adsorbed water in the global water cycle and subsurface ice distribution [11, 12].

MSL recent in situ results at Gale Crater revealed an ubiquitous and diurnally constant Hydrogen signal in ChemCam LIBS spectra of the top μm of the surface [13]. The SAM experiment measured a release of water vapour mostly at high temperatures, indicating a bulk water content of Rocknest's regolith top cm of 1.5-3 wt. %, consistent with tightly bound water molecules [14]. X-ray diffraction spectra reveal that this water is mostly present in the amorphous phase of Rocknest's soil [15].

Here we propose a reassessment of the spatial and temporal distribution of the $3 \mu\text{m}$ absorption distribution and variations using the entire OMEGA dataset, recent laboratory experiments [16, 17] and data processing updates [18].

Data processing and method: We use data from OMEGA imaging spectrometer onboard Mars Express, covering the wavelength range $0.36\text{-}5.1 \mu\text{m}$ and orbiting Mars since 2004. Recent developments by

[19] and validation by [18] allow the use of the long wavelength (covering the $3 \mu\text{m}$ absorption) non-nominal orbits for scientific studies. ~ 6200 OMEGA datacubes were processed for this study, representing more than four full Martian years of orbital data and achieving a global coverage. A specific OMEGA long wavelength channel filtering as well as atmospheric attenuation and thermal contribution corrections have been applied as described in [18]. Water icy frost at the surface have been excluded from this analysis using the $1.5 \mu\text{m}$ band depth described in [18] as well as water ice clouds by the mean of the $3.5 \mu\text{m}$ slope index. OMEGA reflectance spectra are linearized to effective single-particle absorption thickness (ESPAT). Laboratory experiments [16, 17] have revealed that the ESPAT parameter at $2.9 \mu\text{m}$ is linearly correlated to the water content of a set of minerals (montmorillonite, palagonite) with various admixtures of neutral darkening agents. For these samples, the ESPAT parameter at $2.9 \mu\text{m}$ is relatively independent on composition and albedo but still remains strongly dependent on particle size. We use the relationship provided for $<45 \mu\text{m}$ sieved samples because this size fraction is expected to dominate the spectral response of the Martian surface at these wavelengths [5].

Results: The global map of water wt. % is presented in Figure 1 and apparent variations with latitude and season are presented in Figure 2. Previously reported seasonal variations [4, 5] are not observed in the present work. Our water wt. % values are observed to vary with the mineralogical composition: in particular, hydrous minerals appear more hydrated than surrounding terrains and chloride-bearing deposits appear desiccated relatively to surrounding terrains.

The water wt. % distribution of Figure 1 is not correlated to surface particle size proxy such as thermal inertia [18]. Low latitudes ($< 45^\circ$) water wt. % values are not correlated to albedo but high latitudes water wt. % values increase with increasing dust abundance. Apparent seasonal variations of Figure 2 are not attributable to actual changes in surface hydration but rather to seasonally varying atmospheric dust load.

It will be shown that the water wt. % values do not show any conclusive correlation for any type of terrain at any latitude with relative humidity values predicted as a function of time and location by 3D GCM simulations [20].

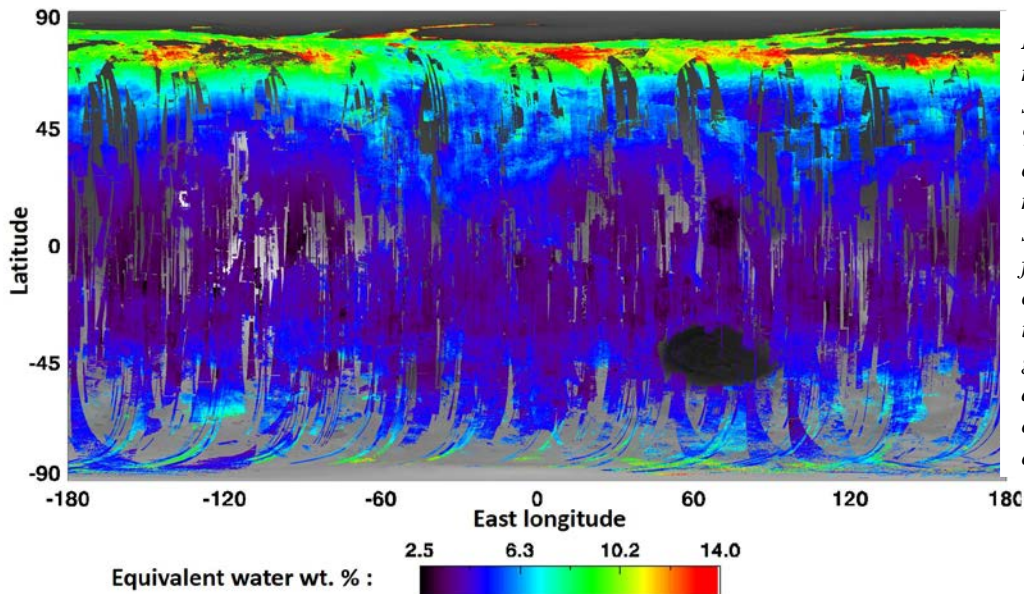


Figure 1. Global map of the optical surface water wt. % at a resolution of 32 ppp. ~400 million OMEGA spectra have been filtered and processed to build this map. A background (model-dependent) level of 4 ± 1 wt. % is observed.

On the other hand, we infer that the increase of surface hydration latitude and the North/South dichotomy could be explained by the long-term action of seasonal water frost and ice deposition at the surface. Since the partial pressure of water vapour is much lower in the southern high latitudes, lower values of surface hydration are indeed expected. Another hint for such a frost-related hydration implementation is the correlation of surface hydration with dust abundance in the high latitudes, as dust provides higher surface of contact of the regolith with the water frost.

Our view of the top surface hydration therefore potentially reveal the process of water implementation into the Martian regolith.

Summary. The apparent hydration of the Martian optical surface seen from orbit :

- Presents a background (model-dependent) level of 4 ± 1 wt. %.
- Varies with latitude, with a non-ambiguous North/South dichotomy.
- Is, for the major part, apparently not exchangeable with the atmosphere on diurnal or seasonal timescales.
- Is stable with regards to the present-day water cycle of Mars, contrarywise to buried hydrogen sources detected by GRS.
- Varies with the mineralogical composition, revealing the importance of structural water.
- Is best explained by the long term action of seasonal water frost and ice deposits at the surface.

These results and the prospective work that they call for will be presented and discussed.

References: [1] Houck J. R. et al. (1973), *Icarus*, 18 (3). [2] Pimmentel G. C. et al. (1974), *JGR*,

79. [3] Bibring J.-P. (1989), *Nature*, 341. [4] Jouglet, D. et al. (2007), *JGR*, 112. [5] Milliken, R. E. et al. (2007), *JGR*, 112. [6] Jakosky, B. M. (1985), *Space Sci. Reviews*, 41. [7] Temppari, L. K. et al. (2010), *JGR*, 115. [8] Maltiagliati, L. et al. (2011), *Icarus*, 213. [9] Montmessin, F. et al. (2004), *JGR*, 109. [10] Böttger, H. M. et al. (2005), *Icarus*, 177. [11] Feldman, W. C. et al. (2004), *JGR*, 109. [12] Schorghofer, N. and Aharonson, O. (2005), *JGR*, 110. [13] Meslin, P.-Y. et al. (2013), *Science*, 341. [14] Leshin, L. A. et al. (2013), *Science*, 341. [15] Bish, D. L. et al. (2013), *Science*, 341. [16] Milliken, R. E. and Mustard, J. (2007a), *Icarus*, 189. [17] Milliken, R. E. and Mustard, J. (2007b), *Icarus*, 189. [18] Audouard, J. et al. (2014), *Icarus*, 233. [19] Jouglet, D. et al. (2009), *Planet and Space Sci.*, 57. [20] Forget, F. et al. (1999), *JGR*, 104.

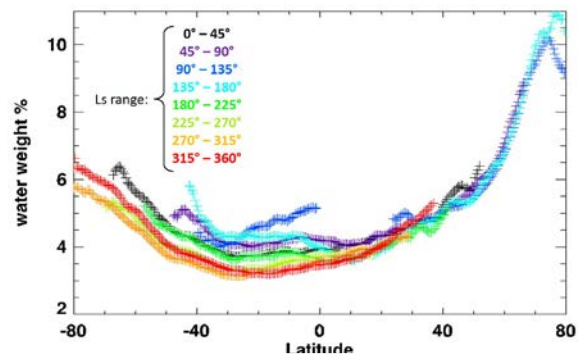


Figure 2. Apparent variations of water wt. % with latitude and season (indicated in different colors). Some residuals of water ice clouds are visible in this plot, for instance at latitude = 10° S for $L_s=90-135^{\circ}$.